atmosphere

MDPI

Article

Analysis of Cross-Polarization Discrimination Due to Rain for Earth–Space Satellite Links Operating at Millimetre-Wave Frequencies in Pretoria, South Africa

Yusuf Babatunde Lawal [1,*], Pius Adewale Owolawi [1], Chunling Tu [1], Etienne Van Wyk [2] and Joseph Sunday Ojo [3]

[1] Department of Computer Systems Engineering, Tshwane University of Technology, Pretoria 0183, South Africa
[2] Faculty of Information and Communications Technology, Tshwane University of Technology, Pretoria 0183, South Africa
[3] Department of Physics, Federal University of Technology, Akure 340110, Nigeria
* Correspondence: lawalyb@tut.ac.za

Abstract: This study investigates the impact of rain-induced attenuation on cross-polarization discrimination (XPD) in Earth–space satellite links operating at millimeter-wave frequencies in Pretoria, South Africa. The traditional method of computing XPD employs a constant annual mean rain height and annual mean co-polar attenuation (CPA) over a certain location. This research utilized seasonal rain height data obtained from a recent study and the latest ITU-R P.618-14 guidelines, to compute and analyze XPD variations across six selected frequencies (11.7 GHz to 35 GHz) for different percentages of time exceedance in Pretoria. The study reveals significant seasonal dependencies of rain heights, with XPD reaching its maximum during winter due to lower rain height, and lower rain-induced attenuation and its minimum during summer, characterized by intense convective rainfall and maximum rain height. For instance, the estimated XPD for a 35 GHz signal at 0.01% of the time in the summer, spring, winter, and autumn are 13, 14, 15, and 14 dB, respectively. This implies that radio signals suffer severe attenuation caused by low XPD in the summer. The relationship between CPA and XPD highlights the need for increased XPD margins at higher frequencies to mitigate signal degradation caused by rain depolarization. Practical recommendations include the adoption of adaptive modulation and coding schemes to maintain link reliability during adverse weather conditions, particularly in summer. This research highlights the significance of incorporating frequency-dependent parameters and rain height variability in XPD estimation to enhance the design of satellite communication systems, ensuring optimized performance and reliable operation in a tropical climate.

Keywords: earth–space links; inter-terrestrial links; millimetre waves; rain height satellite communication; subtropical region; XPD

Academic Editors: Stavros Kolios and Nikos Hatzianastassiou

Received: 12 February 2025
Accepted: 19 February 2025
Published: 24 February 2025

Citation: Lawal, Y.B.; Owolawi, P.A.; Tu, C.; Van Wyk, E.; Ojo, J.S. Analysis of Cross-Polarization Discrimination Due to Rain for Earth–Space Satellite Links Operating at Millimetre-Wave Frequencies in Pretoria, South Africa. *Atmosphere* **2025**, *16*, 256. https://doi.org/10.3390/atmos16030256

1. Introduction

Satellite communication remains an invaluable tool in today's wireless communication systems. This is majorly due to its several merits, especially, the cost-effectiveness and ability to offer the widest coverage when compared to inter-terrestrial links [1–3]. In fact, a constellation of three satellites in the geostationary elliptical orbit (GEO) can provide efficient near-global communication coverage [4–7]. Transmission of radio signals

at frequencies above 10 GHz has several advantages which are able to fulfil modern requirements such as wider spectrum availability, high data transfer rate, and smaller antenna size [8]. Conservation and optimum utilization of frequency is an important factor that must be considered in any satellite communication system because as frequency increases, attenuation due to atmospheric disturbances also increases. To optimize frequency usage in a communication network, frequency reuse is often adopted so that more than one channel per carrier frequency can be transmitted in a communication network. Frequency reuse in satellite communication is enabled by polarization, a method that allows two orthogonally polarized radio waves to be transmitted at a single frequency. Polarization in the context of antenna and radio wave propagation describes how the orientation of an antenna's electric field wave vector aligns relative to the direction of propagation of the electromagnetic waves [9,10]. In radio communication links operating above 10 GHz, frequency reuse in orthogonal polarizations is limited by cross-polarization, a phenomenon where part of a signal originally transmitted in a specific polarization leaks into an orthogonal polarization. Cross-polarization causes a singularly polarized signal to be propagated in two opposite directions, i.e., right hand circular polarization (RHCP) and left hand circular polarization (LHCP) for circularly polarized signal; horizontal and vertical polarization for linearly polarized signal. The reason behind cross-polarization of radio signals in the atmosphere is the presence of hydrometeors such as rain, mist, cloud, snow, and ice. However, rain remains the major cause of severe attenuation and the greatest threat to radio waves propagating at frequencies above 10 GHz in the tropical and subtropical regions [11–13]. These regions experience high-intensity rainfall and longer rainy season compared to other regions. Heavy raindrops are more frequent, leading to scattering and absorption of radio waves [11].

Cross-polarization arises because raindrops are generally non-spherical and can be canted at various angles, causing the polarization plane of electromagnetic waves to rotate and resulting in cross-polarization [14]. The degradation of received signal strength from a singularly polarized wave's quality due to cross-polarization effects is known as CPA. Several studies have shown that cross-polarization occurs because of differential attenuation and differential phase shift between two orthogonal polarizations usually caused by interactions between radio signals and raindrops. Raindrops contribute significantly to the cross-polarization effect when the rain droplet diameter is comparable to the wavelength of radio waves [15–17]. Cross-polarization also increases with increasing frequency, thereby making higher frequency signals more vulnerable. Rain height is a portion along the propagation path shown in Figure 1, where raindrops have significant effects on radio waves, resulting in rain-induced attenuation. It is a function of the melting layer and rain region. The ice region has negligible impacts on radio waves because ice crystals possess very low permittivity and tangent loss [18,19]. Rain heights vary temporally and spatially due to non-uniformity of climate, weather, geological, and topographical formations of satellite–earth receiver stations. The temporal and spatial variation of rain height plays a significant role in the determination of the magnitude of rain-induced attenuation which is responsible for CPA [20–22]. Hence, it is important to consider the impacts of seasonal variation of rain heights and seasonal rain-induced attenuation on CPA in any location. This is because CPA quantifies the loss of power in the co-polarized component due to rain-induced attenuation.

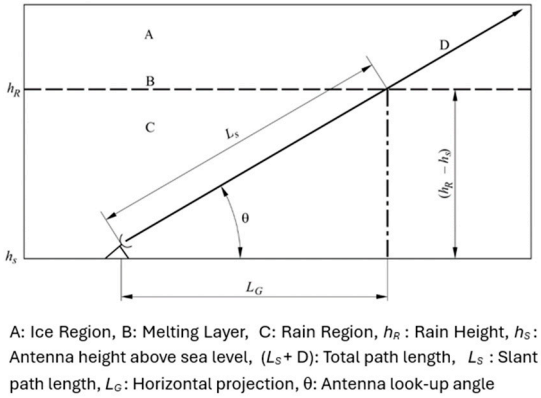

Figure 1. Schematic presentation of an Earth–space path showing rain height and parameters required to compute rain-induced attenuation [23].

Cross-polarization discrimination (XPD) is a parameter used to quantify the ability of a system to distinguish between the desired polarization (co-polarization) and the undesired orthogonal polarization (cross-polarization) [24]. Proper knowledge of XPD due to rain is crucial in wireless networks, especially in dual-polarized satellite communication systems, where one polarization channel is used for transmission and the orthogonal one for reception. Such systems are bound to experience interference between the two channels due to cross-polarization caused mainly by raindrops. The instantaneous XPD of a communication system is greatly influenced by the prevailing CPA, which is a function of the atmospheric conditions. For instance, XPD reduces drastically during heavy thunderstorms due to high CPA and vice versa. As CPA increases due to rain, XPD decreases, leading to potential interference and signal degradation. By understanding and mitigating these effects, system performance can be optimized for reliable communication under varying atmospheric conditions. Hence, it is crucial to estimate the required XPD needed for optimum satellite communication services in any geographical location. The ITU-R P.618 recommendation incorporates polarization effects in satellite link design and acknowledges the advantages of circular polarization in mitigating depolarization and maintaining high XPD values. The recommendation is updated periodically based on recent research findings. The latest version, ITU-R P618-14 [23] was used for this study.

Previous Related Works

Since XPD is a spatio-temporal parameter, several studies have been conducted in many regions to report the statistical estimation of XPD. The impact of rain height variability on XPD in the 10–35 GHz frequency range in India was reported by Sen and Singh [25]. Five years of measured rain height data obtained from the India Meteorological Department were used to compute CPAs and XPDs. The research revealed that CPA varies significantly with rain height, as XPD depends on CPA, frequency, and elevation angle. Lawal et al. [13] utilized kernel density estimation to analyze the spatio-temporal distribution of rain heights in South Africa, revealing seasonal dependencies in rain-induced attenuation. The outcome of the research recommends the use of seasonal rain attenuation values instead of annual mean values in link budget design. Similarly, Mandeep [20] highlighted the variation in XPD in Malaysia, showing that rainstorms in tropical regions exhibit more severe depolarization effects than those in subtropical regions. Ojo [26] studied the relationship between XPD and its dependent parameters such as CPA, frequency, and elevation angle using ITU-R P618-7 [27] in three stations in Nigeria. The research employed fixed annual mean rain heights for the computation of rain-induced attenuation and CPA. It was observed that dual-polarized orthogonal channels operating at a 23° elevation angle are prone to interference due to cross-polarization. Ojo and Owolawi [28] estimated cross-polarization

discrimination due to rain in some stations in South Africa. The research utilized an annual mean rain height to compute rain-induced attenuations for all study locations. Recent research observed significant variation in rain-induced attenuation due to seasonal rain height variability [13]. None of the previous work considered the impacts of seasonal rain height variability on rain-induced attenuation and XPD in Pretoria, which is the major focus of this study. Pretoria, like other areas in South Africa, experiences four distinct weather seasons annually. It has a subtropical climate characterized by warm, wet summers and mild, dry winters. The summer (December–January) is the hottest wet season when most of the annual rainfall occurs. The autumn (March–May) is a transition period with gradually cooling temperatures, while the winter (June–August) is the coldest season characterized by cool, dry weather. The spring (September–November) is a transition season when a gradual rise in temperature signifies the onset of the next summer season. Further details about the climatology and weather of Pretoria can be found in Lawal et al. [13] and Kruger and Nxumalo [29].

2. Methodology

The aim of this study was to investigate the impacts of rain height variability on XPD at some selected frequencies in Pretoria. Seasonal rain heights reported by Lawal et al., [13] in Table 1 were used to compute rain-induced attenuations. The procedure for calculating rain-induced attenuation, which is the major component of CPA, was followed as provided by the most recent ITU-R P618-14 recommendations [23]. The seasonal rain-induced attenuations A_p and CPA (CPA) for various percentages of time p at 11.7 GHz, 15 GHz, 20 GHz, 25 GHz, 30 GHz, and 35 GHz were computed using Pretoria seasonal rain heights and other parameters presented in Table 1 [13]. The recommended seasonal rain heights used for this study were reported in the recent study conducted by Lawal et al. [13] in Pretoria. Frequencies above 10 GHz were selected for the study because the dual polarization method often applied in the frequency reuse technique is usually threatened by cross-polarization effects at these higher frequencies. The 5 GHz interval was adopted to reveal the effects of XPD due to gradual increase in frequency.

Table 1. The Earth station and satellite parameters used for computation of rain-induced attenuation [13,30].

Parameters	Input Values
Ground station latitude	25.542° S
Antenna elevation	31.5°
Antenna height above sea level (m)	1346
1-min rain rate (mm/hr) at 0.01% exceedance	84.5
Autumn rain height (m)	4732
Winter rain height (m)	4308
Spring rain height (m)	4853
Summer rain height (m)	5217
ITU annual mean rain height	4540
Satellite name	IS-20
Polarization	Circular
Satellite position	68.5° E (GEO)

The procedure for the computation of XPD from rain-induced attenuation statistics for earth–space link operating with look-up angle less than 60° is as follows [23].

Step 1: Calculate the frequency-dependent term C_f using Equation (1):

$$C_f = \begin{cases} 60\log f - 28.3 & 6 \le f < 9 \text{ GHz} \\ 26\log f + 4.1 & 9 \le f < 36 \text{ GHz} \end{cases} \quad (1)$$

where f is the frequency in GHz.

Step 2: Calculate the rain attenuation-dependent term C_A:

$$C_A = V(f) log A_p \quad (2)$$

where

$$V(f) = \begin{cases} 30.8 f^{-0.21} & 6 \le f < 9 \text{ GHz} \\ 12.8 f^{0.19} & 9 \le f < 20 \text{ GHz} \\ 22.6 & 20 \le f < 40 \text{ GHz} \end{cases} \quad (3)$$

A_p is the rain-induced attenuation statistics for p percentage of time.

Step 3: Calculate the polarization improvement factor (PIF):

$$C_\tau = -10\log[1 - 0.484(1 + \cos 4\tau)] \quad (4)$$

The improvement factor C_τ = 0 for τ = 45° for circular polarization and reaches a maximum value of 15 dB for τ = 0° or 90°.

Step 4: Calculate the elevation angle-dependent term C_θ:

$$C_\theta = -40\log(cos\theta) \qquad for\ \theta < 60^o \quad (5)$$

where station is the earth station look-up angle also known as path elevation angle.

Step 5: Calculate the canting angle dependent term C_σ:

$$C_\sigma = 0.0053\sigma^2 \quad (6)$$

where σ is the effective standard deviation of the raindrop canting angle distribution, expressed in degrees and it takes the values 0°, 5°, 10°, 15°, and 20° for 1%, 0.1%, 0.01% 0.001%, and 0.0001% of the time, respectively.

Step 6: Calculate XPD_{rain} due to rain not exceeded for p% of the time:

$$XPD_{rain} = C_f - C_A + C_\tau + C_\theta + C_\sigma \quad (7)$$

Analysis of the results obtained are presented and discussed in the subsequent section.

3. Results and Discussion

3.1. Seasonal Variation of XPD at the Selected Frequencies

The seasonal variations of XPD at the 11.7 GHz, 15 GHz, 20 GHz, 25 GHz, 30 GHz, and 35 GHz computed using the seasonal and ITU recommended rain heights Hr are presented in Figure 2a–f, respectively. Generally, the results show that a lower time percentage of signal unavailability results in a decrease in XPD. This implies that an increase in the cross-talk (CPA) would be experienced in the quest to reduce the percentage of signal unavailability during heavy rainy events. Hence, there is a need to maintain a trade-off between XPD and duration of signal outage due to rain-induced attenuation.

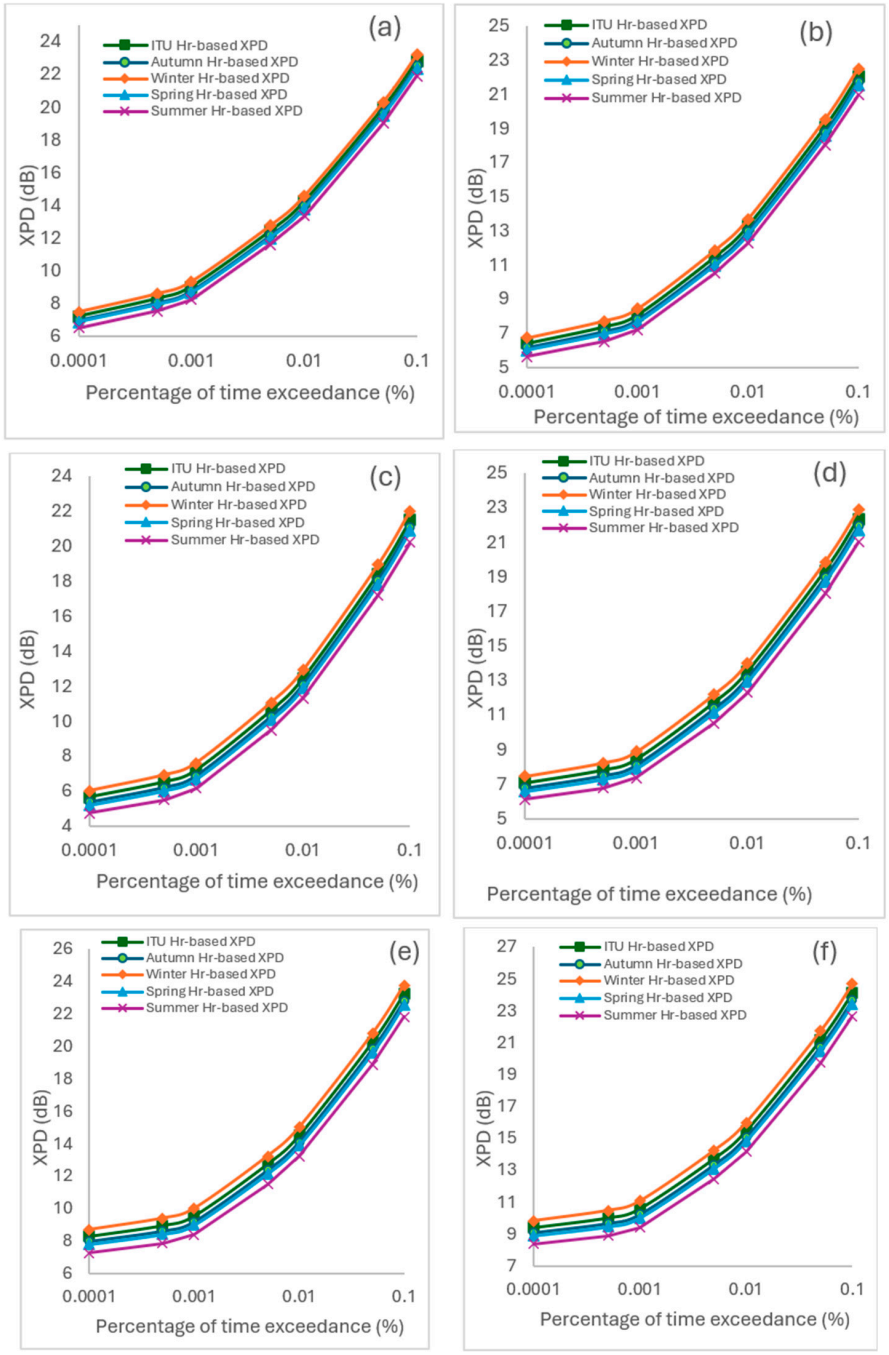

Figure 2. Cumulative distribution of XPD at (**a**) 11.7 GHz, (**b**) 15 GHz, (**c**) 20 GHz, (**d**) 25 GHz, (**e**) 30 GHz, and (**f**) 35 GHz.

The variation in the XPD across the four seasons is evidently influenced by the seasonal rain heights, albeit with minor differences. The curves in Figure 2a–f indicate that XPDs attain minimal values during the summer season at all frequencies. This is because the summer season is a period characterized by frequent convective rainfalls and maximum rain height in Pretoria, during which rain-induced attenuations attain their peak as reported by Lawal et al. [13]. The intense convective rainfall increases rain-induced attenuation, thereby causing a reduction in XPD. The spring season is a transition period when rainfall and rain height reduce gradually, leading to lower attenuation and a consequential increase in XPD. Rain heights and rain-induced attenuation reach the minimal values in the winter, which results in maximum XPDs as depicted in Figure 2a–f. The low values of rain-induced attenuation during the winter and spring indicate rare rainy events that are usually less intense or involve

fewer non-spherical raindrops that could cause depolarization. The maximum XPD, which occurs in the winter, is followed by a gradual decrease during the autumn season, which signifies a transition between the winter and summer. A comparison of the XPD obtained using the annual mean rain height of 4.54 km recommended by ITU with the seasonal XPDs for the study location revealed that the ITU Hr-based XPD slightly underestimates XPD during winter and overestimates during summer, spring, and autumn seasons at various frequencies. These observations agree with the findings of Sen and Singh [25], who applied maximum and minimum rain heights to compute XPD due to rain in Madras, India. From Figure 2a, which presents XPD distribution at 11.7 GHz transmission, it could be observed that at 0.01% of the time, the summer, spring, winter, autumn, and ITU XPDs are 13, 14, 15, 14, and 14 dB, respectively. These represent percentage differences of 7.7%, 0%, 6.7%, and 0% in the summer, spring, winter, and autumn with respect to the ITU XPD of 14 dB. Similarly, at 35 GHz, for the same time percentage of signal unavailability, the summer, spring, winter, autumn, and ITU XPDs are 14, 15, 16, 15, and 16 dB, respectively. These translate to higher percentage differences of 14.3%, 6.7%, 0%, and 6.7% in the summer, spring, winter, and autumn, respectively. The increase in the percentage differences as the frequency increases, especially in the summer, obviously indicates that the effects of rain height variability on XPD are minimal at low frequencies but become significant at higher frequencies.

Statistical comparisons between the seasonal Hr-based XPDs and ITU Hr-based XPDs presented in Table 2 show significant differences at 95% confidence intervals across all the frequencies except for the winter season at 11.7 GHz. The standard deviations of the seasonal XPDs vary between 5.20 and 6.28 across all the frequencies. This underscores the impacts of seasonal variability of rain height on XPD. The seasonal XPDs are, therefore, recommended in the design and optimization of communication links operating above 10 GHz in the study location.

Table 2. Metrics of statistical comparison between seasonal-Hr based XPDs and ITU Hr-based XPD.

Frequency	Season	t-Statistics	*p*-Value	Significance
11.7	Autumn	−4.055	0.0062	Significant
	Winter	2.347	0.0561	Not Significant
	Spring	−4.402	0.0046	Significant
	Summer	−5.673	0.0014	Significant
15	Autumn	−4.250	0.0060	Significant
	Winter	2.890	0.0322	Significant
	Spring	−5.140	0.0024	Significant
	Summer	−6.370	0.0012	Significant
20	Autumn	−4.120	0.0058	Significant
	Winter	2.650	0.0397	Significant
	Spring	−5.080	0.0021	Significant
	Summer	−6.430	0.0008	Significant
25	Autumn	−5.120	0.0023	Significant
	Winter	3.020	0.0231	Significant
	Spring	−6.540	0.0009	Significant
	Summer	−7.320	0.0004	Significant
35	Autumn	−4.310	0.0051	Significant
	Winter	2.890	0.0325	Significant
	Spring	−5.210	0.0027	Significant
	Summer	−6.120	0.0011	Significant

3.2. The Impacts of CPA on XPD

Generally, the XPD varies inversely as the CPA. A radio link with low CPA simply implies that only a tiny component of the total signal is depolarized, hence there is a high discrimination (XPD) between the original polarized and orthogonally polarized waves. Conversely, higher CPA would reduce the XPD, which signifies high cross-talk and a consequential increase in the interference between two orthogonal channels in a communication system. A similar observation was reported for Akure (Nigeria) and Eindhoven (Netherlands) by Ojo [26] and Van de kamp [31], respectively. The observed effects of rain height variability on XPD, especially at high frequencies, informed the decision to investigate the impacts of seasonal CPA on XPD. Figure 3a–d present the relationship between the CPA and the resulting XPD due to rain.

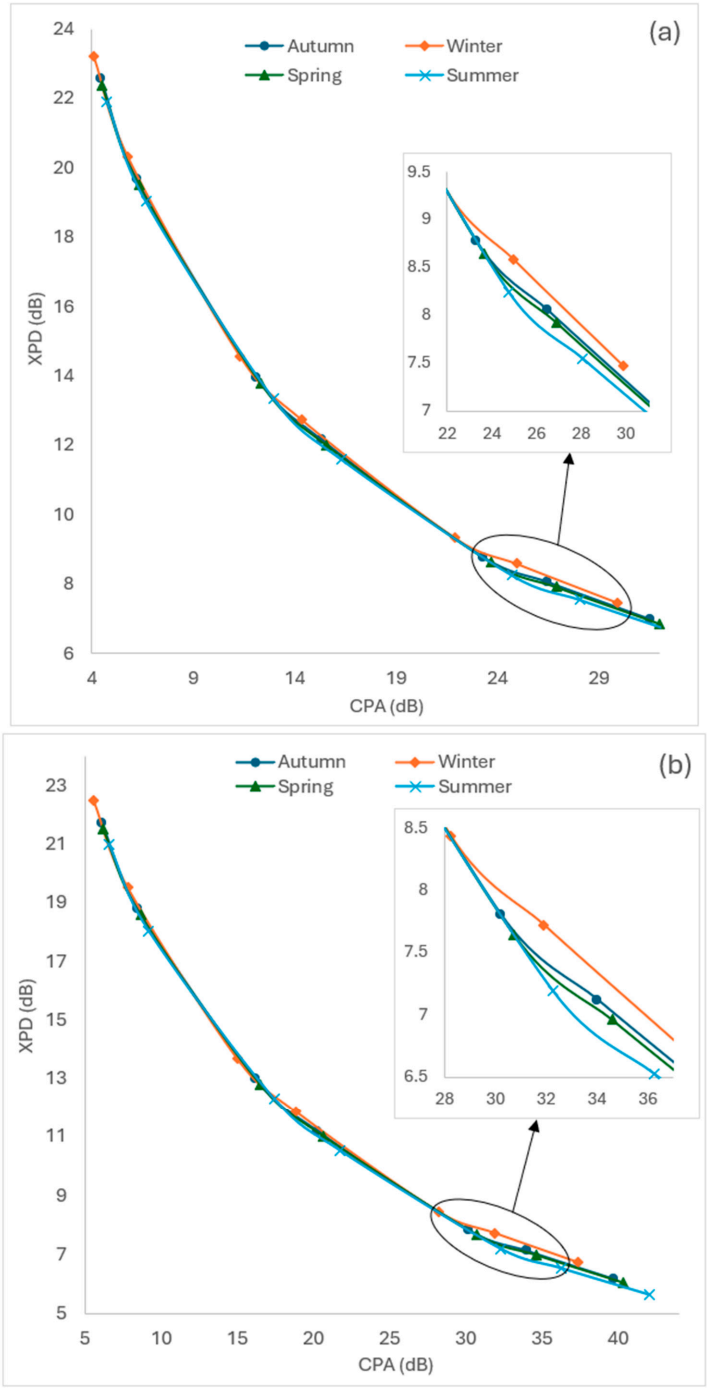

Figure 3. *Cont.*

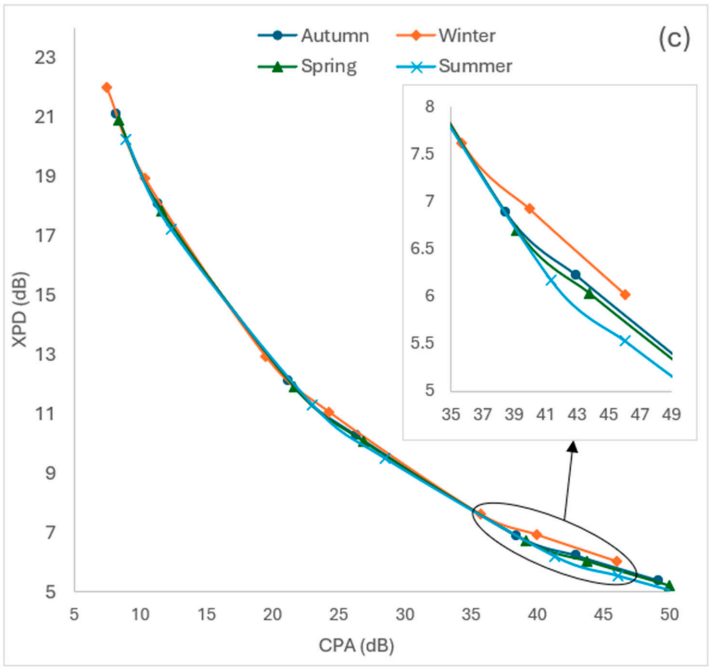

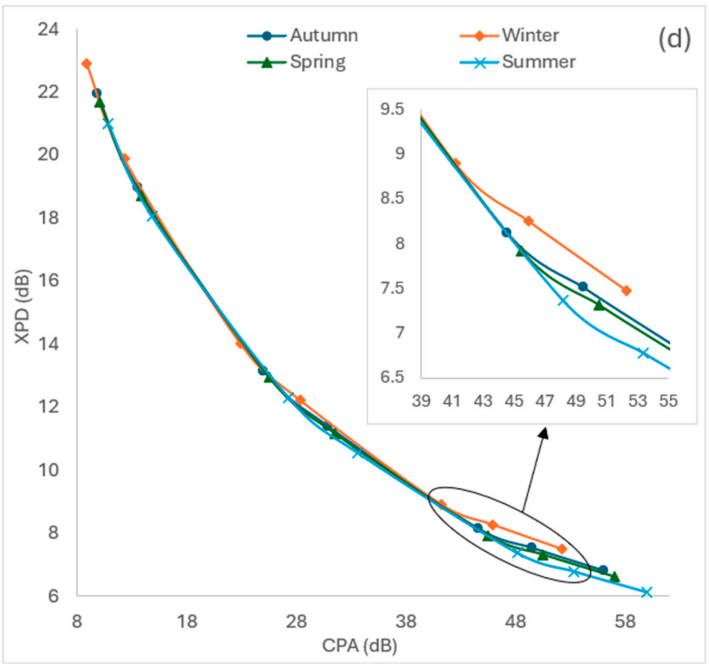

Figure 3. *Cont.*

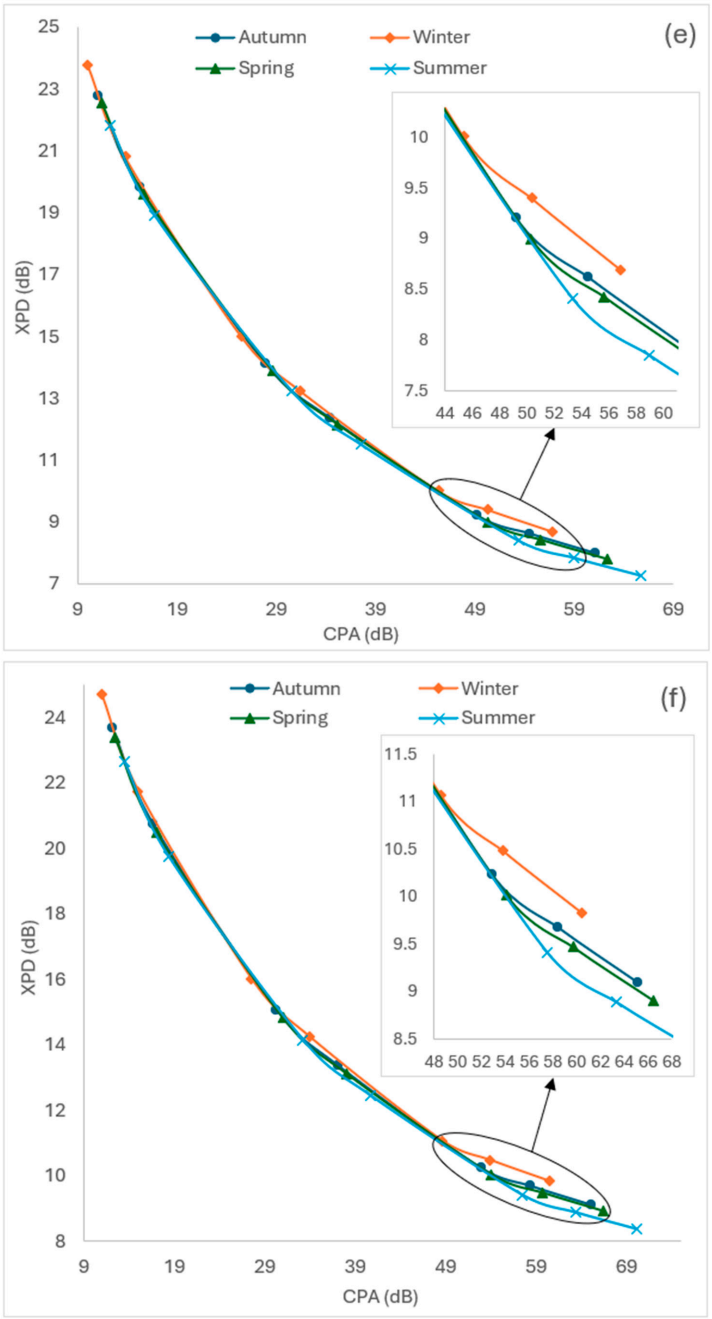

Figure 3. Variation of XPD with CPA (CPA) at (**a**) 11.7 GHz, (**b**) 15 GHz, (**c**) 20 GHz, (**d**) 25 GHz, (**e**) 30 GHz, and (**f**) 35 GHz.

It could be observed from the curves that low values of seasonal CPAs have negligible effects on the seasonal XPD, but notable impacts are evidence at high CPAs. Figure 3a–f show that rain height variability has noticeable impacts on 11.7 GHz, 15 GHz, 20 GHz, 25 GHz, 30 GHz, and 35 GHz radio links when the CPA exceeds 22 dB, 32 dB, 41 dB, 48 dB, 53 dB, and 58 dB, respectively. Hence, special attention must be focused on the XPD of high-frequency signals whose demand is continuously growing due to its several advantages.

3.3. The Impacts of Frequency on XPD at Various Time Percentages

The dynamic relationship between XPD, frequency, and seasonal rain attenuation in Pretoria was also studied. Seasonal rain-induced attenuations at 0.01%, 0.001%, and 0.0001% of time were selected to investigate the effects of frequency on XPD. XPD generally decreases as the frequency increases from 10 GHz to about 20 GHz, showing that maximum

XPD could be attained around 10 GHz as depicted in Figure 4a–d. However, XPD begins to increase with increasing frequency after the dip, resulting in higher values at frequencies above 30 GHz.

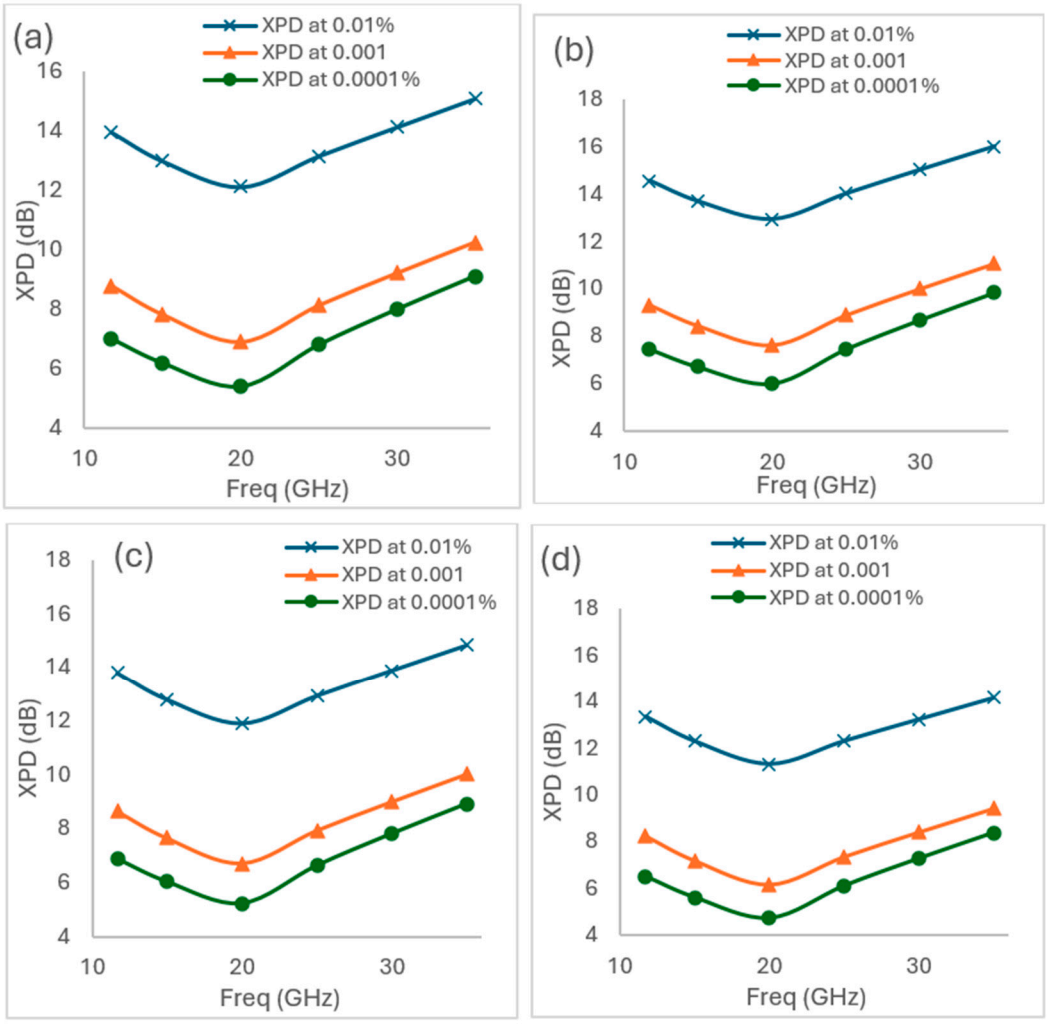

Figure 4. Variation in seasonal XPD with frequency during the: (**a**) autumn (**b**) winter, (**c**) spring, and (**d**) summer.

This trend was observed throughout the seasons, as shown in Figure 4a–d; hence the studied frequencies were divided into three segments. The low-range frequency (10–15 GHz), where XPD is relatively high due to lower rain attenuation and depolarization effects, these frequencies are less affected by non-spherical raindrops that cause depolarization. The mid-range frequency (15–25 GHz) range, where XPD reaches its minimum, indicating significant depolarization caused by rain attenuation. This is consistent with raindrop sizes being comparable to the wavelengths at these frequencies, maximizing depolarization effects. The high-frequency region (>25 GHz), where rain attenuation is higher, and the cross-polarized signal leakage decreases due to reduced scattering effects.

For all seasons, XPD values are higher for lower percentages of time exceedance (e.g., 0.01%) and progressively lower for higher time exceedance percentages (e.g., 0.0001%). This reflects the impact of rain attenuation, as lower percentages of exceedance correspond to severe rainy events, which cause higher depolarization and thus reduce XPD. The values of XPD during autumn are moderate compared to the other seasons. The XPD values for different time percentages are relatively higher compared to summer and spring. This is because autumn rainfall is not as intense as in summer, resulting in less pronounced

depolarization and better XPD. For instance, Table 3 shows that the XPD for 30 GHz at 0.01%, 0.001%, and 0.0001% during the autumn season are 14 dB, 9 dB, and 8 dB while the corresponding values in the summer are 13 dB, 8 dB, and 7 dB, respectively.

Table 3. Seasonal XPDs at different time percentages for the selected frequencies.

Percentage of Time (%)	Frequency (GHz)	XPD (dB)			
		Autumn	Winter	Spring	Summer
0.01	11.7	14	15	14	13
	15	13	14	13	12
	20	12	13	12	11
	25	13	14	13	12
	30	14	15	14	13
	35	15	16	15	14
0.001	11.7	9	9	9	8
	15	8	8	8	7
	20	7	8	7	6
	25	8	9	8	7
	30	9	10	9	8
	35	10	11	10	9
0.0001	11.7	7	8	7	7
	15	6	7	6	6
	20	5	6	5	5
	25	7	8	7	6
	30	8	9	8	7
	35	9	10	9	8

The winter season has the highest XPD across all time percentages and frequencies as shown in Table 3. Although the minimum XPD occurs around 20 GHz, it is not as low as other seasons. XPD values in spring exhibits similar behaviour to autumn but with slightly lower overall values, especially at lower time percentages. Spring rain patterns likely involve lighter but more frequent rainfall, contributing to moderate depolarization effects. XPD remains lowest in summer with a steep reduction for higher time percentages, especially around 20 GHz.

3.4. Practical Implications of XPD Variability for Satellite Communication Systems and Recommendations

Satellite communication links, therefore, appear most greatly challenged during the summer because of the lowest XPD in Pretoria, especially during heavy rain events. This implies that the quality of radio signals is heavily attenuated due to low XPD in the summer. Winter conditions are the most favourable because XPD reaches its peak and depolarization is relatively low. It was found that seasonal XPD is more reliable, hence it can be used in high availability systems at frequencies around 10–15 GHz. Margin or adaptive modulation must be used for mid-range frequency (15–25 GHz) due to problems with rain depolarization. Satellite systems that employ the Ka and higher frequency bands (>25 GHz) require a higher XPD but also consider the increased rain attenuation at these bands. In the case of lower XPD values, adaptive modulation and coding schemes are suggested for optimal performance during summer months. Bandwidth of both options should be increased and adopted during winter months only, to provide the best link performance at the highest XPD. Link budgeters ought to assume lossier polarization isolation schemes for mid-range frequencies (15–25 GHz) where depolarization conditions are most dramatic.

4. Conclusions

This study examined the effects of seasonal variation of rain heights on relevant radio propagation parameters for circularly polarized Earth–space satellite links in Pretoria. The results showed that XPD varies directly with percentage of time exceedance and reduces as frequency and co-polar attenuation levels increase. However, XPD starts declining at frequencies higher than 20 GHz, which demonstrates the intricate links between frequency and polarization effects. This implies that communication system design requires attention to rain height variation caused by seasonal changes which contributes to signal degradation and depolarization. This study revealed that XPD achieves peak values in winter and minimum values in summer seasons, while spring and autumn seasons maintained moderate values at all the selected frequencies. Sufficient XPD must be provided for radio signals operating above 25 GHz to compensate for depolarization caused by heavy raindrops. The deployment of adaptive modulation and coding techniques in summer months is recommended to boost link reliability because they improve system performance in changing atmospheric conditions. Development and application of the recommended depolarization mitigation techniques in the study location are recommended for further research.

Author Contributions: Conceptualization, Y.B.L. and P.A.O.; methodology, Y.B.L.; software, Y.B.L., C.T. and P.A.O.; validation, Y.B.L. and P.A.O.; formal analysis, Y.B.L., C.T. and J.S.O.; investigation, Y.B.L.; resources, C.T. and E.V.W.; data curation, Y.B.L.; writing—original draft preparation, Y.B.L.; writing—review and editing, Y.B.L., P.A.O. and J.S.O.; visualization, Y.B.L. and J.S.O.; supervision, P.A.O., C.T. and J.S.O.; project administration, C.T. and E.V.W.; funding acquisition, Y.B.L. and E.V.W. All authors have read and agreed to the published version of the manuscript.

Funding: This research was funded by Tshwane University of Technology in South Africa.

Institutional Review Board Statement: Not applicable.

Informed Consent Statement: Not applicable.

Data Availability Statement: The sources of the data used for this research are provided in the Section 2.

Conflicts of Interest: The authors declare no conflicts of interest.

References

1. Sadiku, M.N.O. Satellite Communication Systems. In *Handbook of Engineering Electromagnetics*, 1st ed.; Bansal, R., Ed.; CRC Press: Boca Raton, FL, USA, 2004; pp. 16-1–16-24. [CrossRef]
2. Chuberre, N.; Cote, J.; Bruniera, J.J.; Benard, P.; Potuaud, D. Satellite Communication System for a Continuous High-Bitrate Access Service over a Coverage Area Including at Least One Polar Region. U.S. Patent 9,363,712, 7 June 2016.
3. Tripathi, N.; Sharma, K.K.; Pandey, U. Analytical review on satellite communication: Benefits, issues, and future challenges. In *Computer Aided Constellation Management and Communication Satellites*; Singh, D., Chaudhary, R.K., Dev Kumar, K., Eds.; Lecture Notes in Electrical Engineering; Springer: Singapore, 2023; Volume 987, pp. 235–258. [CrossRef]
4. Lang, T.J.; Adams, W.S. A comparison of satellite constellations for continuous global coverage. In *Mission Design & Implementation of Satellite Constellations: Proceedings of an International Workshop*; Springer: Dordrecht, The Netherlands, 1998; pp. 51–62. [CrossRef]
5. Wang, B.; Wang, J.; Wang, X.; Gao, H.; Wang, M.; Li, H. Design Method for Realizing Flexible Coverage of Global Communication Constellation. CN111800182B, 18 May 2021.
6. Dou, Y.; Liu, X. Design of global coverage satellite constellation based on GEO and IGSO. In *Communications, Signal Processing, and Systems*; Springer: Singapore, 2020. [CrossRef]
7. The European Space Agency (ESA). Types of Orbit. Available online: https://www.esa.int/Enabling_Support/Space_Transportation/Types_of_orbits (accessed on 2 December 2024).
8. Pi, Z.; Khan, F. An introduction to millimeter-wave mobile broadband systems. *IEEE Commun. Mag.* **2011**, *49*, 101–107. [CrossRef]
9. Stutzman, W.L.; Thiele, G.A. *Antenna Theory and Design*, 3rd ed.; Wiley: Hoboken, NJ, USA, 2012.
10. Balanis, C.A. *Antenna Theory: Analysis and Design*, 4th ed.; Wiley: Hoboken, NJ, USA, 2016.

11. Azmi, M.H.; Rahman, T.A.; Islam, M.R. Rain attenuation measurements and analysis at 73 GHz E-band link in tropical region. *IEEE Access* **2020**, *8*, 123456–123465. [CrossRef]
12. Mandeep, J.S.; Hassan, S.I.S. Rain attenuation prediction models for terrestrial microwave links. *J. Atmos. Sol.-Terr. Phys.* **2015**, *123*, 61–73. [CrossRef]
13. Lawal, Y.B.; Owolawi, P.A.; Tu, C.; Van Wyk, E.; Ojo, J.S. The kernel density estimation technique for spatio-temporal distribution and mapping of rain heights over South Africa: The effects on rain-induced attenuation. *Atmosphere* **2024**, *15*, 1354. [CrossRef]
14. Singh, A.; Meena, R.S. Assessment of dual-polarized interference due to rain-induced depolarization in satellite communication links. *SN Appl. Sci.* **2020**, *2*, 989. [CrossRef]
15. Balakrishna, P.; Bindu, G.R.; Thomas, J. Rain-induced cross-polarization at cm and mm wavelengths. *Indian J. Radio Space Phys.* **1999**, *28*, 159–164.
16. Sen Jaiswal, R.; Geetha, P.; Uma, S. Estimation of cross-polarization due to rain over some stations in India. *Indian J. Space Radio Phys.* **2007**, *36*, 379–382.
17. Durodola, O.M.; Aminu, I.; Ojo, J.S.; Ajewole, M.O. Investigation of Depolarization and Cross Polarization over Ku-band Satellite Links in a Guinea Savanna Location, Nigeria. In Proceedings of the URSI Atlantic Radio Science Conference, Gran Canaria, Spain, 28 May–1 June 2018. Available online: https://www.ursi.org/proceedings/procAT18/papers/CrossPolarizationonKuLinksJournal.pdf (accessed on 10 December 2024).
18. Plummer, D.M. Discrimination of mixed- versus ice-phase clouds using dual-polarization radar with application to detection of aircraft icing regions. *J. Appl. Meteorol. Climatol.* **2010**, *49*, 920–936. [CrossRef]
19. Oguchi, T. Electromagnetic wave propagation and scattering in rain and other hydrometeors. *Proc. IEEE* **1983**, *71*, 1029–1078. [CrossRef]
20. Mandeep, J.S. Rain height statistics for satellite communication in Malaysia. *J. Atmos. Sol.-Terr. Phys.* **2008**, *70*, 1617–1620. [CrossRef]
21. Nzeako, A.N.; Falowo, O.E. Impact of rain height on rain-induced attenuation on satellite links in tropical regions. *IEEE Trans. Antennas Propag.* **2017**, *65*, 3516–3525.
22. Lawal, Y.B.; Ojo, J.S.; Falodun, S.E. Variability and trends in rain height retrieved from GPM and implications on rain-induced attenuation over Nigeria. *Heliyon* **2021**, *7*, e08108. [CrossRef]
23. *ITU-R, P.618-14*; Propagation Data and Prediction Methods Required for the Design of Earth-Space Telecommunication Systems. International Telecommunication Union; Radiocommunication Section (ITU-R): Geneva, Switzerland, 2023.
24. Lim, Y.-G.; Cho, Y.J.; Oh, T.; Lee, Y.; Chae, C.-B. Relationship between cross-polarization discrimination (XPD) and spatial correlation in indoor small-cell MIMO systems. *IEEE Wirel. Commun. Lett.* **2018**, *7*, 392–395. [CrossRef]
25. Sen, R.; Singh, M.P. Estimation of cross polarization of millimeter waves due to rain over few stations in India and its modification incorporating measured values of rain height. In Proceedings of the 6th International Symposium on Antennas, Propagation and EM Theory (ISAPE), Beijing, China, 28 October–1 November 2003; pp. 568–571. [CrossRef]
26. Ojo, J.S. Estimation of cross-polarization due to rain over some stations in Nigeria. *Ann. Telecommun* **2012**, *67*, 241–245. [CrossRef]
27. *ITU-R, P.618-7*; Propagation Data and Prediction Methods Required for the Design of Earth-Space Telecommunication Systems. International Telecommunication Union: Geneva, Switzerland, 2007.
28. Ojo, J.S.; Owolawi, P.A. Statistical studies of cross-polarization due to subtropical rain on SHF radio propagation paths over some stations in South Africa. *Wirel. Pers. Commun.* **2017**, *95*, 1725–1735. [CrossRef]
29. Kruger, A.C.; Nxumalo, M.P. Historical rainfall trends in South Africa: 1921–2015. *Water SA* **2017**, *43*, 285–297. [CrossRef]
30. Lawal, Y.B.; Owolawi, P.A.; Tu, C.; Van Wyk, E.; Ojo, J.S. Performance of advanced-deep learning algorithm for modeling and prediction of rain height over some selected locations in the tropics and sub-tropics zone for radio propagation applications. *Edelweiss Appl. Sci. Technol.* **2024**, *8*, 520–537. [CrossRef]
31. Van de Kamp, M.M.J.L. Depolarization due to rain: The XPD–CPA relation. In Proceedings of the IEEE Antennas and Propagation Society International Symposium (APS), Orlando, FL, USA, 11–16 July 1999; pp. 400–403. [CrossRef]